For JAXA R&D

PPP - Models, Algorithms and Implementations (4)

Tokyo Univ. of Marine Science and Technology (TUMSAT)

Tomoji TAKASU

2019-11-22 @Tokyo, Japan

PPP - Models, Algorithms and Implementation

1. 2019-10-04 **PPP models**
   geometric range, ionosphere, troposphere, antenna PCV, earth tides, wind-up, relativity, biases, coordinates
2. 2019-10-18 **PPP algorithms**
   SPP, LSQ, GN, EKF, noise-model, RAIM/QC, LAPACK/BLAS
3. 2019-11-01 **PPP data handling**
   LC, interpolation, slip detection, RINEX, SP3, ANTEX, RTCM, CSSR
4. 2019-11-22 **PPP-AR**
   UPD/FCB, EWL/WL/NL, ILS, LAMBDA, TCAR, PAR, validation
5. 2019-12-06 **INS integration**
   INS sensors, Inertial navigation, INS integration
6. 2019-12-20 **POD of satellites**
   orbit element, orbit model, reduced-dynamic, ECI-ECEF transformation, precession/nutation, EOP

(1.5 h / session)

Notations

c	: Speed of light (m/s)
P^s_{r,L_i}	: L_i Peudorange measurement (m)
φ^s_{r,L_i}	: L_i Carrier phase measurement (cyc)
Φ^s_{r,L_i}	: L_i Phase-range measurement (m)
t_r	: Signal reception time (s)
t^s	: Signal transmission time (s)
ρ^s_r	: Geometric range (m)
$\mathbf{r}^s(t)$	: Satellite position in ECEF (m)
$\mathbf{v}^s(t)$	: Satellite velocity in ECEF (m)
$\mathbf{r}_r$	: Receiver position in ECEF (m)
$\mathbf{e}^s_r$	: LOS vector in ECEF
$\mathbf{e}^s_{r,enu}$	: LOS vector in local coordinates
ϕ_r	: Latitude of receiver position (rad)
λ_r	: Longitude of receiver position (rad)
h_r	: Ellipsoidal height of receiver (m)
H_r	: Orthometric height of receiver (m)
Az^s_r	: Azimuth angle of satellite (rad)
El^s_r	: Elevation angle of satellite (rad)
dt_r	: Receiver clock bias (s)
$dT^s(t)$	: Satellite clock bias (s)
I^s_r	: Ionospheric delay (m)
T^s_r	: Tropospheric delay (m)
f_i	: L_i carrier frequency (Hz)
λ_i	: L_i carrier wavelength (m)
B^s_{r,L_i}	: L_i Carrier phase bias (m)
N^s_{r,L_i}	: L_i Carrier phase ambiguity (cyc)
ε_P	: Code measurement error (m)
ε_Φ	: Phase measurement error (m)
ω_e	: Earth rotation velocity (rad/s)
Z_t	: Zenith total delay (m)
Z_h	: Zenith hydrostatic delay (m)
Z_w	: Zenith wet delay (m)
$m_h(El)$	: Hydrostatic mapping function
$m_w(El)$	: Wet mapping function
$\mathbf{U}(t)$	: ECEF to ECI transformation matrix
$\mathbf{E}_r$	: ECEF to local coordinates rotation matrix
$\mathbf{E}^s$	: ECEF to satellite body rotation matrix
$\mathbf{R}_x(\theta)$	: Coordinates rotation matrix around X
$\mathbf{R}_y(\theta)$	: Coordinates rotation matrix around Y
$\mathbf{R}_z(\theta)$	: Coordinates rotation matrix around Z

Ambiguity Resolution

(AR)

Ambiguity Resolution (AR)

Objectives of AR

More accurate solutions after proper AR (FIXED vs. FLOAT)

Faster solution convergence, ideally FIXED instantaneously

Carrier phase observables can be handled as precise pseudorange after AR

Initial phase terms should be eliminated for AR

Both of satellite and receiver initial phases do not have integer nature

DD (double difference) used for baseline processing like RTK

ZD (zero-difference) carrier-phase

$$\Phi_r^s = \rho_r^s + c(dt_r - dT^s(t^s)) - I_r^s + T_r^s + d_r^s + \lambda d_{pw} + \lambda(\phi_{r,0} - \phi_0^s + N_r^s) + \varepsilon_\Phi$$

DD (double-difference) carrier-phase for baseline processing

$$\Phi_{rb}^{ij} = \rho_{rb}^{ij} - I_{rb}^{ij} + T_{rb}^{ij} + d_{rb}^{ij} + \lambda d_{pw,rb}^{ij} + \lambda N_{rb}^{ij} + \varepsilon_\Phi$$

$$\Phi_{rb}^{ij} \approx \rho_{rb}^{ij} + \lambda N_{rb}^{ij} + \varepsilon_\Phi \quad \text{(short-baseline, same antenna)}$$

$()^{ij}$: Difference between satellite i and j

$()_{rb}$: Difference between receiver r and b

N_r^s : Integer ambiguity (cyc)

ϕ_0^s : Satellite initial phase (cyc)

$\phi_{r,0}$: Receiver initial phase (cyc)

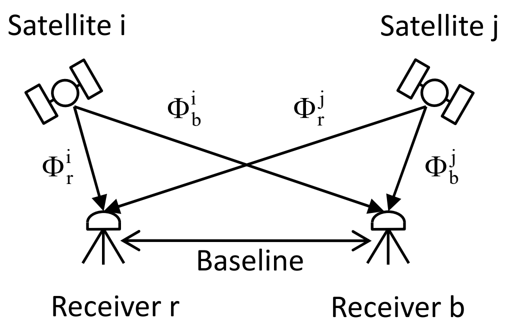

FIXED Solution with AR

Typical AR Steps [1]

(1) $\mathbf{y} = \mathbf{Hx} + \boldsymbol{\varepsilon} = \mathbf{Aa} + \mathbf{Bb} + \boldsymbol{\varepsilon} \quad \left(\mathbf{a} \in \mathbf{Z}^n, \mathbf{b} \in \mathbf{R}^p\right)$ Mixed-integer measurement models

(2) $\hat{\mathbf{x}} = \begin{pmatrix} \hat{\mathbf{a}} \\ \hat{\mathbf{b}} \end{pmatrix}, \mathbf{Q}_{\hat{\mathbf{x}}} = \begin{pmatrix} \mathbf{Q}_{\hat{\mathbf{a}}} & \mathbf{Q}_{\hat{\mathbf{a}}\hat{\mathbf{b}}} \\ \mathbf{Q}_{\hat{\mathbf{b}}\hat{\mathbf{a}}} & \mathbf{Q}_{\hat{\mathbf{b}}} \end{pmatrix}$ FLOAT solution and VC matrix by LSE or KF

(3) $\hat{\mathbf{a}} \rightarrow \breve{\mathbf{a}}$ Mapping FLOAT to FIXED

(4) $\breve{\mathbf{b}} = \hat{\mathbf{b}} - \mathbf{Q}_{\hat{\mathbf{b}}\hat{\mathbf{a}}} \mathbf{Q}_{\hat{\mathbf{a}}}^{-1} (\hat{\mathbf{a}} - \breve{\mathbf{a}})$ FIXED solution

Mapping FLOAT to FIXED ($\hat{\mathbf{a}} \rightarrow \breve{\mathbf{a}}$)

Integer Rounding (IR)

$$\breve{\mathbf{a}} = [\hat{\mathbf{a}}] = \left([\hat{a}_1], [\hat{a}_2], \ldots, [\hat{a}_n]\right)^T$$

Integer Bootstrapping (conditional sequential rounding) (IB)

$$\breve{\mathbf{a}} = \left([\hat{a}_1], \left[\hat{a}_2 - \sigma_{21}\sigma_1^{-2}(\hat{a}_1 - \breve{a}_1)\right], \ldots, \left[\hat{a}_n - \sum_{i=1}^{n-1} \sigma_{n,i|I}\sigma_{i|I}^{-2}(\hat{a}_{i|I} - \breve{a}_i)\right] \right)^T$$

Integer Least Squares (ILS)

$$\breve{\mathbf{a}} = \underset{\mathbf{a} \in \mathbf{Z}}{\arg\min} \left(\hat{\mathbf{a}} - \mathbf{a}\right)^T \mathbf{Q}_{\hat{\mathbf{a}}}^{-1} \left(\hat{\mathbf{a}} - \mathbf{a}\right)$$

$\mathbf{a}$: Integer ambiguity parameters

$\mathbf{b}$: Other parameters

$\hat{\mathbf{a}}, \hat{\mathbf{b}}$: FLOAT solutions

$\breve{\mathbf{a}}, \breve{\mathbf{b}}$: FIXED solutions

$[x]$: Rounding to the nearest integer

$$\mathbf{Q}_{\hat{\mathbf{a}}} = \begin{pmatrix} \sigma_1^2 & \sigma_{12} & \cdots & \sigma_{1n} \\ \sigma_{21} & \sigma_2^2 & \cdots & \sigma_{2n} \\ \vdots & \vdots & \ddots & \vdots \\ \sigma_{n1} & \sigma_{n2} & \cdots & \sigma_n^2 \end{pmatrix}$$

[1] P. J. G. Teunissen and O. Montenbruck (eds.), Springer Handbook of Global Navigation Satellite Systems, 2017, Springer, Section 23

AR by ILS

AR Techniques based on ILS [1]

Technique	Reference	Ambiguity Search Method	Data Processing Method	Search Space Handling Method	Note
LSAST	Hatch, 1990	Independent	Single-epoch	None	Least-Squares Ambiguity Search Technique
FARA	Frei and Beutler, 1990	All	Multi-epoch	Conditional	Fast Ambiguity Resolution Approach
Modified Cholesky Decomposition	Euler and Landau, 1992	All	Multi-epoch	None	
LAMBDA	Teunissen, 1994	All	Multi-epoch	Transformation/ Conditional	Least-squares AMBiguity Decorrelation Adjustment
Null Space	Martin-Neira, 1995	Independent	Single-epoch	Transformation	
FASF	Chen and Lachapelle, 1995	All	Multi-epoch	Conditional	Fast Ambiguity Search Filter
OMEGA	Kim and Langley, 1999	Independent	Single/ Multi-epoch	Transformation/ Conditional	Optimal Method for Estimating GPS Ambiguities

[1] D. Kim and B. Langley, GPS Ambiguity Resolution and Validation: Methodologies, Trends and Issues, 7th Workshop International Symposium on GPS/GNSS, 2000

LAMBDA

Least-squares AMBiguity Decorrelation Adjustment [1]

A GNSS AR strategy by ILS estimator

Shrinking integer search space with "decorrelation"

Skillful and efficient tree search strategy

Similar to "Closest Point Search with LLL Lattice Basis Reduction" Algorithm [2]

$$\breve{\mathbf{a}} = \arg\min_{\mathbf{a}\in \mathbf{Z}^n} (\hat{\mathbf{a}}-\mathbf{a})^{\mathrm{T}} \mathbf{Q}_{\hat{\mathbf{a}}}^{-1}(\hat{\mathbf{a}}-\mathbf{a})$$

$$\breve{\mathbf{a}} = \mathbf{Z}^{-\mathrm{T}}\breve{\mathbf{z}}$$

Z-transformation

$$\hat{\mathbf{z}} = \mathbf{Z}^{\mathrm{T}}\hat{\mathbf{a}},\ \mathbf{Q}_{\hat{\mathbf{z}}} = \mathbf{Z}^{\mathrm{T}}\mathbf{Q}_{\hat{\mathbf{a}}}\mathbf{Z}$$

$$\breve{\mathbf{z}} = \arg\min_{\mathbf{z}\in \mathbf{Z}^n} (\hat{\mathbf{z}}-\mathbf{z})^{\mathrm{T}} \mathbf{Q}_{\hat{\mathbf{z}}}^{-1}(\hat{\mathbf{z}}-\mathbf{z})$$

$$(\hat{\mathbf{z}}-\mathbf{z})^{\mathrm{T}}\mathbf{Q}_{\hat{\mathbf{z}}}^{-1}(\hat{\mathbf{z}}-\mathbf{z}) = (\mathbf{Z}^{\mathrm{T}}\hat{\mathbf{a}}-\mathbf{Z}^{\mathrm{T}}\mathbf{a})^{\mathrm{T}}\left(\mathbf{Z}^{\mathrm{T}}\mathbf{Q}_{\hat{\mathbf{a}}}\mathbf{Z}\right)^{-1}(\mathbf{Z}^{\mathrm{T}}\hat{\mathbf{a}}-\mathbf{Z}^{\mathrm{T}}\mathbf{a})$$

$$= (\hat{\mathbf{a}}-\mathbf{a})^{\mathrm{T}}\mathbf{Z}\left(\mathbf{Z}^{-1}\mathbf{Q}_{\hat{\mathbf{a}}}^{-1}\mathbf{Z}^{-\mathrm{T}}\right)\mathbf{Z}^{\mathrm{T}}(\hat{\mathbf{a}}-\mathbf{a}) = (\hat{\mathbf{a}}-\mathbf{a})^{\mathrm{T}}\mathbf{Q}_{\hat{\mathbf{a}}}^{-1}(\hat{\mathbf{a}}-\mathbf{a})$$

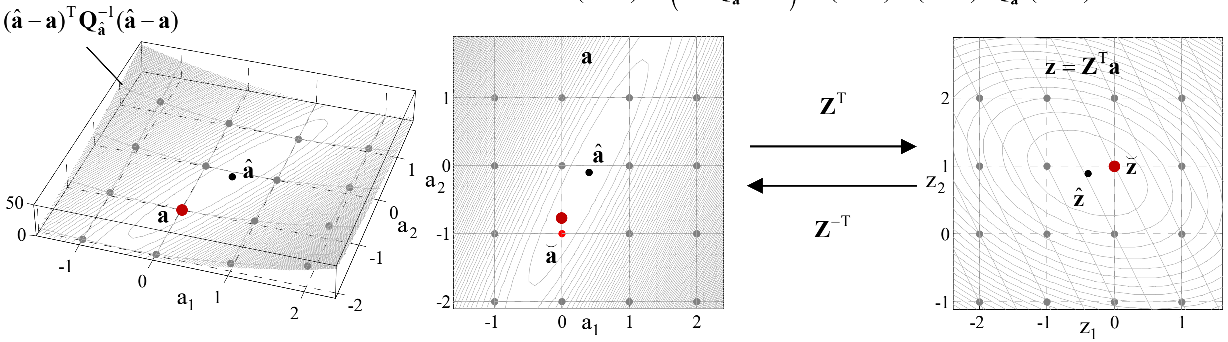

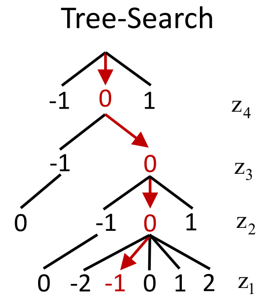

[1] P. J. G. Teunissen, The least-squares ambiguity decorrelation adjustment: a method for fast GPS integer ambiguity estimation. Journal of Geodesy, 1994

[2] E. Agrell, Closest point search in lattices, IEEE Transaction on Information Theory, 2002

CPU Time for LAMBDA

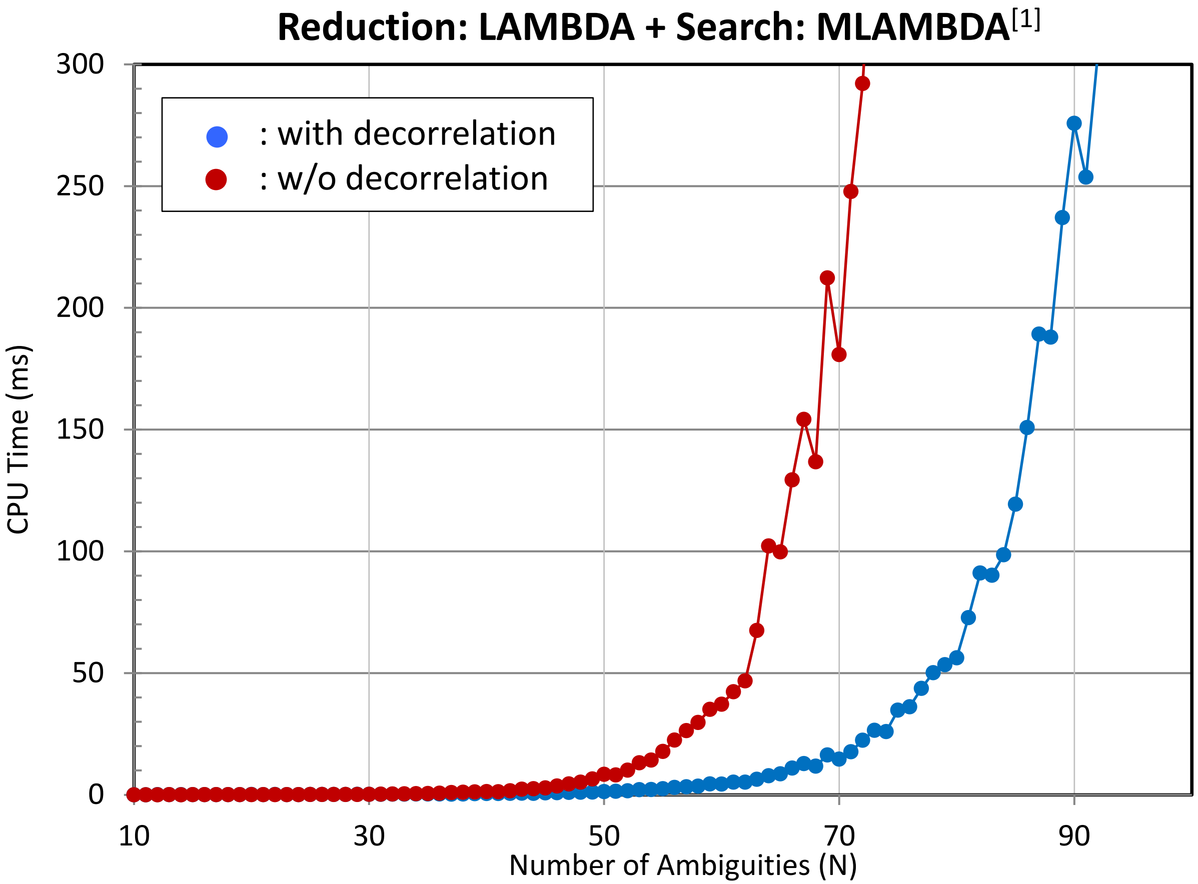

(Core i7 5960X, 3.0-3.5 GHz, RTKLIB 2.4.2, gcc 5.4.0, σ_y = 0.03 cyc)

[1] X. -W. Chang, X. Yang and T. Zhou, MLAMBDA: A modified LAMBDA method for integer least-squares estimation, Journal of Geodesy, 2005

Validation of AR

Acceptance Test after AR

- Wrong AR much degrades the quality of the final (FIXED) solution
- Need to maximize AR success probability and to minimize AR failure rate
- Remain ambiguities FLOAT if the acceptance test failed and output FLOAT solution instead
- Several acceptance tests are proposed: [1]

Ratio Test

$$\text{accept } \breve{\mathbf{a}} \text{ if : } \frac{\|\hat{\mathbf{a}} - \breve{\mathbf{a}}'\|^2_{\mathbf{Q}_{\hat{\mathbf{a}}}}}{\|\hat{\mathbf{a}} - \breve{\mathbf{a}}\|^2_{\mathbf{Q}_{\hat{\mathbf{a}}}}} \geq c$$

Difference Test

$$\text{accept } \breve{\mathbf{a}} \text{ if : } \|\hat{\mathbf{a}} - \breve{\mathbf{a}}'\|^2_{\mathbf{Q}_{\hat{\mathbf{a}}}} - \|\hat{\mathbf{a}} - \breve{\mathbf{a}}\|^2_{\mathbf{Q}_{\hat{\mathbf{a}}}} \geq c$$

F-Ratio Test

$$\text{accept } \breve{\mathbf{a}} \text{ if : } \frac{\|\hat{\mathbf{e}}\|^2_{\mathbf{Q}_{\mathbf{y}}} + \|\hat{\mathbf{a}} - \breve{\mathbf{a}}'\|^2_{\mathbf{Q}_{\hat{\mathbf{a}}}}}{\|\hat{\mathbf{e}}\|^2_{\mathbf{Q}_{\mathbf{y}}} + \|\hat{\mathbf{a}} - \breve{\mathbf{a}}\|^2_{\mathbf{Q}_{\hat{\mathbf{a}}}}} \geq c$$

Projector Test

$$\text{accept } \breve{\mathbf{a}} \text{ if : } \left| \frac{(\breve{\mathbf{a}}' - \breve{\mathbf{a}})^T \mathbf{Q}_{\hat{\mathbf{a}}}^{-1} (\hat{\mathbf{a}} - \breve{\mathbf{a}})}{\|\breve{\mathbf{a}}' - \breve{\mathbf{a}}\|^2_{\mathbf{Q}_{\hat{\mathbf{a}}}}} \right| \leq \mu$$

$\breve{\mathbf{a}}'$: Second-best candidate of AR, c, μ : Test thresholds $\|\mathbf{x}\|^2_{\mathbf{Q}} = \mathbf{x}^T \mathbf{Q}^{-1} \mathbf{x}$ $\hat{\mathbf{e}} = \mathbf{y} - \mathbf{A}\hat{\mathbf{a}} - \mathbf{B}\hat{\mathbf{b}}$

Note: The test thresholds are usually selected empirically as a fixed value (for example Ratio Test with c = 3). The threshold value, however, is often optimistic or conservative without theoretical basis.
In some literatures, variable threshold values are proposed base on fixed-failure rate approach (FF-RT) [2].

[1] S. Verhagen and P. J. G. Teunissen, New global navigation satellite system ambiguity resolution method compared to exiting approaches, Journal of Guidance, Control and Dynamics, 2006

[2] S. Verhagen and P. J. G. Teunissen, The ratio test for future GNSS ambiguity resolution, GPS Solution, 2013

Partial AR (PAR)

Partial AR (PAR)

- Full AR (FAR) indicates low fixing ratio or long TTFF under ill conditions like long BL RTK
- Newly rising satellites or cycle-slips often disturbs FAR with validation
- Degraded accuracy by PAR solutions acceptable in many applications

Many criteria how to select subset of ambiguities:

- Elevation angle, continuous tracking epochs, SNR, ADOP (ambiguity dilution of precision), EWL/WL/NL, success or failure probability of AR

BSR (bootstrapping success rate) Criterion [1]

$$\prod_{i=k}^{n}\left(2\Phi\left(\frac{1}{2\sigma_{\hat{z}_{i|I}}}\right)-1\right) \ge P_0$$

P_0 : Minimum success probability of bootstrapping AR

$\sigma_{\hat{z}_{i|I}}$: Std-dev of Z-transformed i-th ambiguity of bootstrapping AR

$\Phi(x)$: CDF (cumulative distribution function) of normal distribution

FF-RT (fixed-failure-rate ratio-test) Criterion [1]

$$\frac{\left\|\hat{\mathbf{z}}_p - \breve{\mathbf{z}}'_p\right\|^2_{\mathbf{Q}_{\hat{z}_p}}}{\left\|\hat{\mathbf{z}}_p - \breve{\mathbf{z}}_p\right\|^2_{\mathbf{Q}_{\hat{z}_p}}} \ge c(n, P_f)$$

$p = (k, k+1, \ldots, n)$: Partial set of Z-transformed ambiguities

$\hat{\mathbf{z}}_p$: Float Z-transformed ambiguities

$\breve{\mathbf{z}}_p, \breve{\mathbf{z}}'_p$: Best-fixed, secondary-best-fixed Z-transformed ambiguities

$c(n, P_f)$: Threshold of FF-RT (fixed-failure-rate ratio-test)

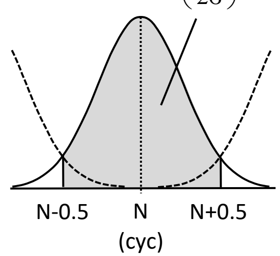

$$2\Phi\left(\frac{1}{2\sigma}\right)-1$$

$$\Phi(x) = \frac{1}{\sqrt{2\pi}}\int_{-\infty}^{x}\exp\left(-\frac{t^2}{2}\right)dt = \frac{1}{2}\left(1-\mathrm{erf}\left(\frac{1}{\sqrt{2}}\right)\right)$$

[1] S. Verhagen et al., GNSS ambiguity resolution: which subset to fix ?, International GNSS Symposium, 2011

WL/NL AR with Iono-free LC

FLOAT Solution and LC Ambiguity *

$$\mathbf{x} = (\mathbf{r}_r^T, T, \mathbf{N}_{LC}^T)^T, \mathbf{y} = (\mathbf{P}_{LC}^T, \mathbf{\Phi}_{LC}^T)^T, \mathbf{Q}_\mathbf{y}$$

$$\begin{cases} P_{LC} = C_1 P_{L1} + C_2 P_{L2} = \rho + mT + \varepsilon_P \\ \Phi_{LC} = C_1 \Phi_{L1} + C_2 \Phi_{L2} = \rho + mT + N_{LC} + \varepsilon_\Phi \end{cases}$$

$$\rightarrow \hat{\mathbf{x}} = (\hat{\mathbf{r}}_r^T, \hat{T}, \hat{\mathbf{N}}_{LC}^T)^T, \mathbf{Q}_{\hat{\mathbf{x}}}$$

FLOAT WL Ambiguity *

$$\hat{N}_{WL} = \frac{1}{n}\sum_{i=1}^{n}(MW) = \frac{1}{n}\sum_{i=1}^{n}(\Phi_{WL} - P_{NL})$$
$$= \frac{1}{n}\sum_{i=1}^{n}\left(\left(\frac{\Phi_{L1}}{\lambda_1} - \frac{\Phi_{L2}}{\lambda_2}\right) - \left(\frac{P_{L1}}{\lambda_1} + \frac{P_{L2}}{\lambda_2}\right)\right)$$

Ionosphere-free

geometry-free,
Ionosphere-free

WL/NL AR by IR **

$$\breve{N}_{WL} = \left[\hat{N}_{WL}\right] \quad \text{(WL AR)}$$

$$\breve{N}_{L1} = \left[\hat{N}_{L1}\right] = \left[\frac{\hat{N}_{LC} - C_2\lambda_2\breve{N}_{WL}}{\lambda_{NL}}\right] \quad \text{(NL AR)}$$

FIXED Solution *

$$\mathbf{x} = (\mathbf{r}_r^T, T)^T, \mathbf{y} = (\mathbf{\Phi}_{LC}^T)^T$$

$$\Phi_{LC} = C_1 \Phi_{L1} + C_2 \Phi_{L2} = \rho + mT + \breve{N}_{LC} + \varepsilon_\Phi$$

$$\rightarrow \breve{\mathbf{x}} = (\breve{\mathbf{r}}_r^T, \breve{T})^T, \mathbf{Q}_{\breve{\mathbf{x}}}$$

N_{LC} : Iono-free LC ambiguity (m)
N_{WL} : Wide lane ambiguity (cyc)
m : Mapping function
T : ZTD or ZWD (m)

$$C_1 = \frac{\lambda_2^2}{\lambda_2^2 - \lambda_1^2}, C_2 = \frac{-\lambda_1^2}{\lambda_2^2 - \lambda_1^2}$$

$$C_1\lambda_1 + C_2\lambda_2 = \frac{\lambda_1\lambda_2}{\lambda_1 + \lambda_2} = \frac{1}{1/\lambda_1 + 1/\lambda_2} = \lambda_{NL}$$

$$N_{WL} = N_{L1} - N_{L2}$$

$$N_{LC} = C_1\lambda_1 N_{L1} + C_2\lambda_2 N_{L2} = (C_1\lambda_1 + C_2\lambda_2)N_{L1} - C_2\lambda_2 N_{WL}$$
$$= \lambda_{NL} N_{L1} - C_2\lambda_2 N_{WL}$$

Note:

* DD applied for baseline processing to eliminate clock and initial bias terms. SD applied for PPP-AR with FCB corrections

** Alternatively, ILS or IB can be applied to NL AR considering the VC-matrix of FLOAT LC ambiguities

L1/L2 AR with STEC Estimation

FLOAT Solution, STEC and L1/L2 Ambiguity * ***

$$\mathbf{x} = (\mathbf{R}^T, \mathbf{N}^T)^T, \mathbf{y} = (\mathbf{P}_{L1}^T, \mathbf{P}_{L2}^T, \mathbf{\Phi}_{L1}^T, \mathbf{\Phi}_{L2}^T)^T, \mathbf{Q}_\mathbf{y}$$

$$\begin{cases} P_{L1} = \rho + I + mT + \varepsilon_P \\ P_{L2} = \rho + \gamma I + mT + \varepsilon_P \\ \Phi_{L1} = \rho - I + mT + \lambda_1 N_{L1} + \varepsilon_\Phi \\ \Phi_{L2} = \rho - \gamma I + mT + \lambda_2 N_{L2} + \varepsilon_\Phi \end{cases} \qquad \begin{pmatrix} \mathbf{R} = (\mathbf{r}_r^T, T, \mathbf{I}^T)^T \\ \mathbf{N} = (\mathbf{N}_{L1}^T, \mathbf{N}_{L2}^T)^T \end{pmatrix}$$

$$\rightarrow \hat{\mathbf{x}} = (\hat{\mathbf{R}}^T, \hat{\mathbf{N}}^T)^T, \mathbf{Q}_{\hat{\mathbf{x}}} = \begin{pmatrix} \mathbf{Q}_{\hat{\mathbf{R}}} & \mathbf{Q}_{\hat{\mathbf{N}}\hat{\mathbf{R}}} \\ \mathbf{Q}_{\hat{\mathbf{R}}\hat{\mathbf{N}}} & \mathbf{Q}_{\hat{\mathbf{N}}} \end{pmatrix}$$

L1/L2 AR by ILS **

$$\breve{\mathbf{N}} = \underset{\mathbf{N} \in \mathbf{Z}^n}{\arg\min} \left(\hat{\mathbf{N}} - \mathbf{N}\right)^T \mathbf{Q}_{\hat{\mathbf{N}}}^{-1} \left(\hat{\mathbf{N}} - \mathbf{N}\right)$$

FIXED Solution

$$\breve{\mathbf{R}} = (\breve{\mathbf{r}}_r^T, \breve{T}, \breve{\mathbf{I}}^T)^T = \hat{\mathbf{R}} - \mathbf{Q}_{\hat{\mathbf{R}}\hat{\mathbf{N}}} \mathbf{Q}_{\hat{\mathbf{N}}}^{-1} (\hat{\mathbf{N}} - \breve{\mathbf{N}})$$

I : Slant ionospheric delay (STEC) at L1 frequency (m) $\quad \gamma = (\lambda_2 / \lambda_1)^2$

Note:

* DD applied for baseline processing to eliminate clock and initial bias terms. SD applied for PPP-AR with FCB corrections

** PAR instead of FAR could be applied to improve fixing ratio and TTFF

*** It is easily enhanced to triple or quad frequency measurements

TCAR/CIR

TCAR (three-carrier AR) [1] /CIR (cascade integer resolution) [2]

Sequential conditional rounding EWL -> WL -> NL ambiguities

Geometry-free measurement model

Ionosphere terms can be reduced by short baseline or ionosphere corrections (for PPP)

Many modifications or enhancements including geometry-based models

$$(1)\ \breve{N}_{EWL} = \left[\frac{\Phi_{EWL} - P_X}{\lambda_{EWL}}\right]$$

$$(2)\ \breve{N}_{WL} = \left[\frac{\Phi_{WL} - (\Phi_{EWL} - \lambda_{EWL}\breve{N}_{EWL})}{\lambda_{WL}}\right]$$

$$(3)\ \breve{N}_{NL} = \left[\frac{\Phi_{NL} - (\Phi_{WL} - \hat{N}_{WL})}{\lambda_{NL}}\right]$$

$$\begin{cases} P_X = \rho + I_X + T + \varepsilon_P \\ \Phi_{EWL} = \rho - I_{EWL} + T + \lambda_{EWL} N_{EWL} + \varepsilon_{\Phi_{EWL}} \\ \Phi_{WL} = \rho - I_{WL} + T + \lambda_{WL} N_{WL} + \varepsilon_{\Phi_{WL}} \\ \Phi_{NL} = \rho - I_{NL} + T + \lambda_{NL} N_{NL} + \varepsilon_{\Phi_{NL}} \end{cases}$$

$$|I_X + I_{EWL}| \ll \lambda_{EWL}, |I_{WL}| \ll \lambda_{WL}, |I_{NL}| \ll \lambda_{NL}$$

Typical Selection of EWL, WL and NL for GPS

$$P_X = \frac{P_{L2}/\lambda_2 + P_{L5}/\lambda_5}{1/\lambda_2 + 1/\lambda_5}, \Phi_{EWL} = \frac{\Phi_{L2}/\lambda_2 - \Phi_{L5}/\lambda_5}{1/\lambda_2 - 1/\lambda_5}, \Phi_{WL} = \frac{\Phi_{L1}/\lambda_1 - \Phi_{L2}/\lambda_2}{1/\lambda_1 - 1/\lambda_2}, \Phi_{NL} = \Phi_{L1}$$

[1] U. Vollath et al., Analysis of three-carrier ambiguity resolution (TCAR) technique for precise relative positioning in GNSS-2, ION GPS-98

[2] J. Jung and P. Enge, Optimization of cascade integer resolution with three civil GPS frequency, ION GPS 2000

Triple Frequency LC

$$\Phi_{(i,j,k)} = \frac{i/\lambda_1\Phi_{L1} + j/\lambda_2\Phi_{L2} + k/\lambda_5\Phi_{L5}}{i/\lambda_1 + j/\lambda_2 + k/\lambda_5} \qquad P_{(l,m,n)} = \frac{l/\lambda_1 P_{L1} + m/\lambda_2 P_{L2} + n/\lambda_5 P_{L5}}{l/\lambda_1 + m/\lambda_2 + n/\lambda_5}$$

Type	LC	Coefficients						λ_{LC} (cm)	I_{LC} (wrt P1)	σ_{LC}		Note
		i	j	k	l	m	n			(cm)	(cyc)	
Geometry Based	$\Phi_{(1,0,0)}$	1	-	-	-	-	-	19.0	-1	0.3	0.016	NL
	$\Phi_{(0,1,0)}$	-	1	-	-	-	-	24.4	-1.647	0.3	0.012	NL
	$\Phi_{(0,0,1)}$	-	-	1	-	-	-	25.5	-1.793	0.3	0.012	NL
	$\Phi_{(1,-1,0)}$	1	-1	-	-	-	-	86.1	1.283	1.7	0.020	WL
	$\Phi_{(1,0,-1)}$	1	-	-1	-	-	-	75.1	1.339	1.5	0.020	WL
	$\Phi_{(0,1,-1)}$	-	1	-1	-	-	-	586.1	1.719	10.0	0.017	EWL
	$\Phi_{(1,-6,5)}$	1	-6	5	-	-	-	325.6	0.074	31.1	0.096	EWL
	$\Phi_{(1,-5,4)}$	1	-5	4	-	-	-	209.3	0.662	16.5	0.079	EWL
	$\Phi_{(4,-3,0)}$	4	-3	-	-	-	-	11.4	-0.090	0.8	0.073	NL
	$\Phi_{(4,0,-3)}$	4	-	-3	-	-	-	10.8	0.010	0.8	0.072	NL
Geometry Free	$\Phi_{(1,-1,0)} - P_{(1,1,0)}$	1	-1	-	1	1	-	86.1	0	21.4	0.249	WL
	$\Phi_{(1,0,-1)} - P_{(1,0,1)}$	1	-	-1	1	-	1	75.1	0	21.5	0.286	WL
	$\Phi_{(0,1,-1)} - P_{(0,1,1)}$	-	1	-1	-	1	1	586.1	0	23.4	0.040	EWL
	$\Phi_{(1,-6,5)} - P_{(1,1,1)}$	1	-6	5	1	1	1	325.6	-1.360	35.7	0.110	EWL
	$\Phi_{(1,-6,5)} - P_{(1,1,0)}$	1	-6	5	1	1	-	325.6	-1.209	37.8	0.116	EWL
	$\Phi_{(1,-5,4)} - P_{(1,1,1)}$	1	-5	4	1	1	1	209.3	-0.773	24.1	0.115	EWL
	$\Phi_{(1,-5,4)} - P_{(1,1,0)}$	1	-5	4	1	1	-	209.3	-0.622	27.0	0.129	EWL

$$\lambda_{LC} = \frac{1}{i/\lambda_1 + j/\lambda_2 + k/\lambda_5} \qquad N_{LC} = i\cdot N_{L1} + j\cdot N_{L2} + k\cdot N_{L5} \qquad I_{LC} = -\frac{i/\lambda_1 + j\cdot\lambda_2/\lambda_1^2 + k\cdot\lambda_5/\lambda_1^2}{i/\lambda_1 + j/\lambda_2 + k/\lambda_5} - \frac{l/\lambda_1 + m\cdot\lambda_2/\lambda_1^2 + n\cdot\lambda_5/\lambda_1^2}{l/\lambda_1 + m/\lambda_2 + n/\lambda_5}$$

$$\sigma_{LC} = \sqrt{\frac{(i/\lambda_1)^2 + (j/\lambda_2)^2 + (k/\lambda_5)^2}{(i/\lambda_1 + j/\lambda_2 + k/\lambda_5)^2}\sigma_\Phi^2 + \frac{(l/\lambda_1)^2 + (m/\lambda_2)^2 + (n/\lambda_5)^2}{(l/\lambda_1 + m/\lambda_2 + n/\lambda_5)^2}\sigma_P^2} \qquad (\sigma_\Phi = 0.3\text{cm},\ \sigma_P = 30\text{cm})$$

PPP-AR

PPP-AR

PPP (w/o AR)

Developed by JPL in 1990s to facilitate the analysis of large reference station N/W data [1]

Conventionally PP (post processing) with IGS precise ephemeris

AR has been difficult due to unknown satellite initial phase term

$$\Phi_r^s = \rho_r^s + c(dt_r - dT^s(t^s)) - I_r^s + T_r^s + d_r^s + \lambda d_{pw} + \lambda(\phi_{r,0} \boxed{- \phi_0^s} + N_r^s) + \varepsilon_\Phi$$

Satellite initial phase

PPP-AR (PPP with AR)

Many research works have been done to introduce AR for PPP

- Based on FCB (fractional cycle bias) or UPD (uncalibrated phase delay) [2]
- Based on IRC (integer recovery clock) or decoupled clock model [3]
- Based on globally estimated phase ambiguities in reference station N/W [4]

Recently PPP-AR is enhanced to RT (real-time) [5] and multi-constellation GNSS

Commercial PPP Services based on PPP-AR

Several services have been already launched since 2000s

[1] J. F. Zumberge et al., Precise Point Positioning for the efficient and robust analysis of GPS data from large networks, Journal of Geophysical Research, 1997

[2] M. Ge et al., Resolution of GPS carrier-phase ambiguities in Precise Point Positioning (PPP) with daily observation, Journal of Geodesy, 2008

[3] P. Collins et al., Precise Point Positioning with ambiguity resolution using the decoupled clock model, ION ITM 2008

[4] W. Bertiger et al., Single receiver phase ambiguity resolution with GPS data, Journal of Geodesy, 2010

[5] D. Laurichesse et al., Real time-difference ambiguities fixing and absolute RTK, ION NTM 2008

RT PPP-AR

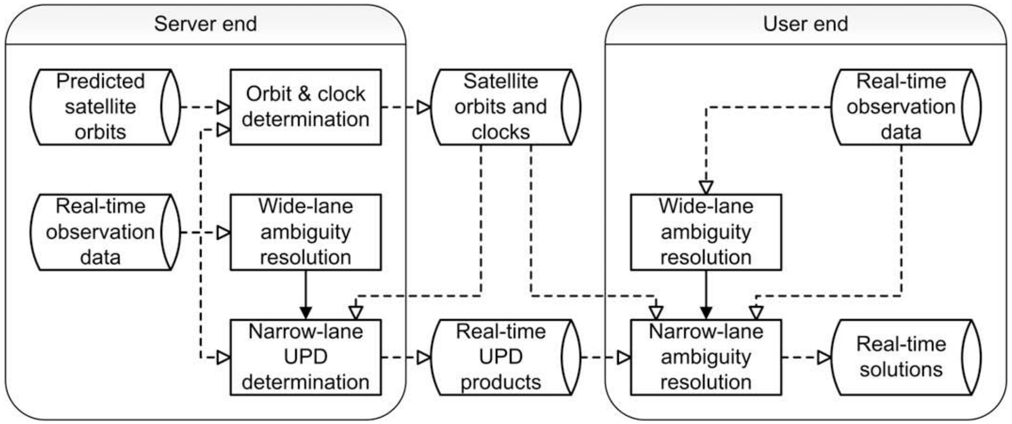

FLOAT Solutions

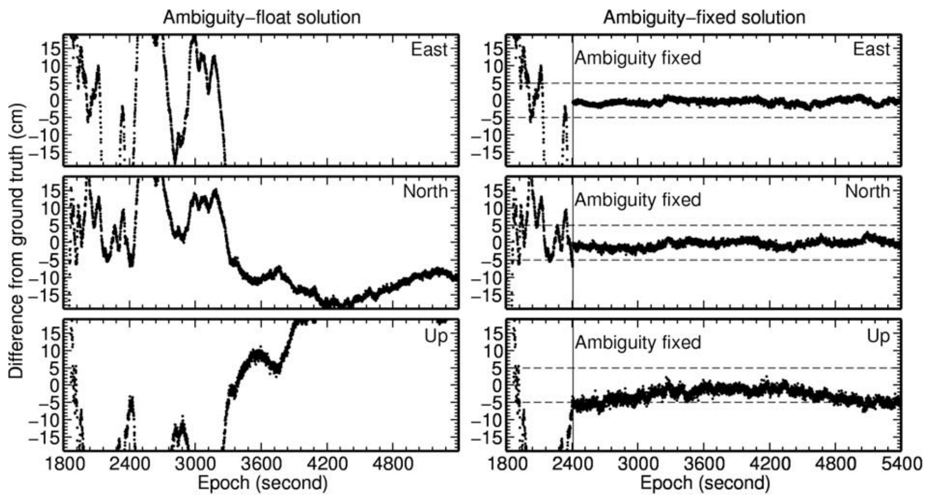

FIXED Solutions

[1] J. Geng et al., Towards PPP-RTK: Ambiguity resolution in real-time precise point positioning, Advances in Space Research, 2010

FCB/UPD Generation

Generate SD-Ambiguity

$$\hat{B}^{i,j}_{k,XL} = \left(\hat{B}^{i}_{k,XL} - \hat{B}^{j}_{k,XL}\right)/\lambda_{XL}$$

Average SD-FCB [(A)]

$$b^{i,j}_{XL} = \frac{1}{n}\sum_{k=1}^{n}\left(\left(\hat{B}^{i,j}_{k,XL} - b_0\right) - \left[\hat{B}^{i,j}_{k,XL} - b_0\right]\right) + b_0$$

- XL : Ambiguity type (NL/WL/EWL/L1/2/5)
- i,j : Satellite
- k : Receiver in ref stations N/W
- $\hat{B}^{i}_{k,XL}$: Estimated float ambiguity (m)
- $\hat{N}^{i,j}_{k,XL}$: SD-float ambiguity (cyc)
- $b^{i,j}_{XL}$: SD-FCB (cyc)
- b^{i}_{XL} : ZD-FCB (cyc)
- b_0 : Initial SD-FCB (cyc)
- $\mathbf{D}$: ZD to SD transformation matrix ($\mathbf{b}_{SD} = \mathbf{D}\mathbf{b}_{ZD}$)

FCB SD-to-ZD Decomposition

$$\mathbf{b}_{SD} = \left(b^{1,2}_{XL},\dots,b^{1,m}_{XL},b^{2,3}_{XL},\dots,b^{2,m}_{XL},\dots,b^{m-1,m}_{XL}\right)^T$$

$$\mathbf{b}_{ZD} = \left(b^{1}_{XL},b^{2}_{XL},\dots,b^{m}_{XL}\right)^T = \left(\left(\mathbf{D}^T,\mathbf{1}\right)\left(\mathbf{D}^T,\mathbf{1}\right)^T\right)^{-1}\left(\mathbf{D}^T,\mathbf{1}\right)\left(\mathbf{b}^T_{SD},0\right)^T$$

FCB Validation

$$N = \hat{B}^{i,j}_{k,XL} - (b^{i}_{XL} - b^{i}_{XL})$$

if $\left|N - [N]\right| > \delta N_{max}$ **or** $P_N(N,\sigma_B) < P_{N,min}$ **, reject** $\hat{B}^{i,j}_{k,XL}$ **and goto (A), end**

NL/WL/EWL -> L1/L2/L5 [1]

$$b^{i}_{L1} = b^{i}_{NL} - b^{i}_{WL}\cdot\lambda_1/(\lambda_2-\lambda_1)$$

$$b^{i}_{L2} = b^{i}_{NL} - b^{i}_{WL}\cdot\lambda_2/(\lambda_2-\lambda_1)$$

$$b^{i}_{L5} = b^{i}_{L2} - b^{i}_{EWL}$$

$$P_N(N,\sigma_N) = 1 - \sum_{n=1}^{nmax}\left(\mathrm{erfc}\left(\frac{n-\left|N-[N]\right|}{\sqrt{2}\sigma_N}\right) - \mathrm{erfc}\left(\frac{n+\left|N-[N]\right|}{\sqrt{2}\sigma_N}\right)\right)$$

: Confidence function of ambiguity

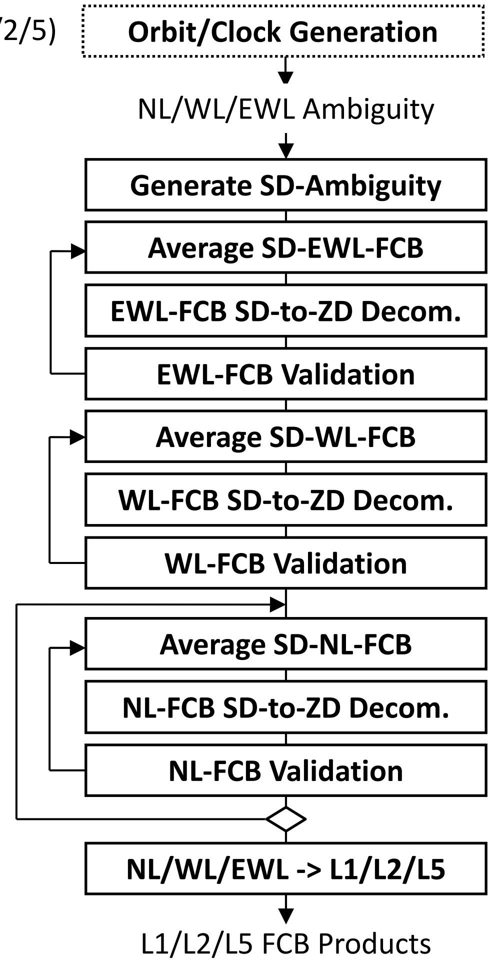

[1] X. Li et al., A method for improving uncalibrated phase delay estimation and ambiguity-fixing in real-time precise point positioning, Journal of Geodesy, 2013

FCB/UPD Examples

WL-FCB (2014/10/1 - 2015/3/31)

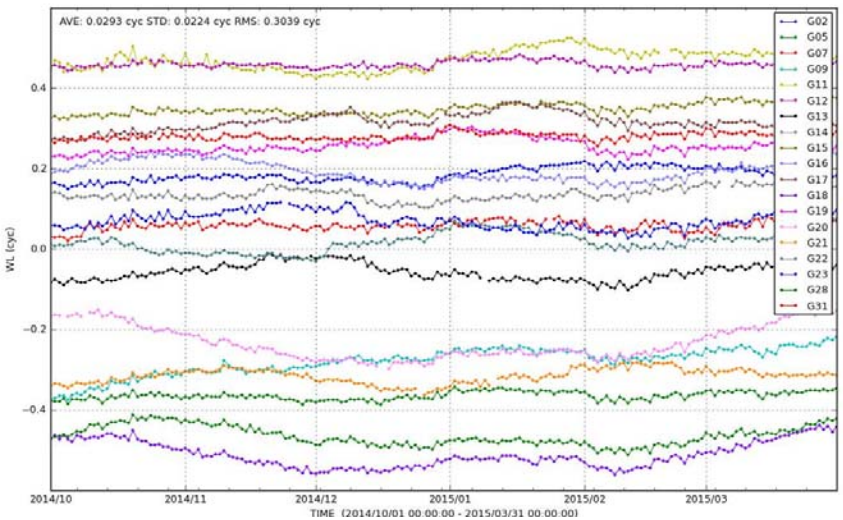

NL-FCB (2014/10/1 - 2014/10/31)

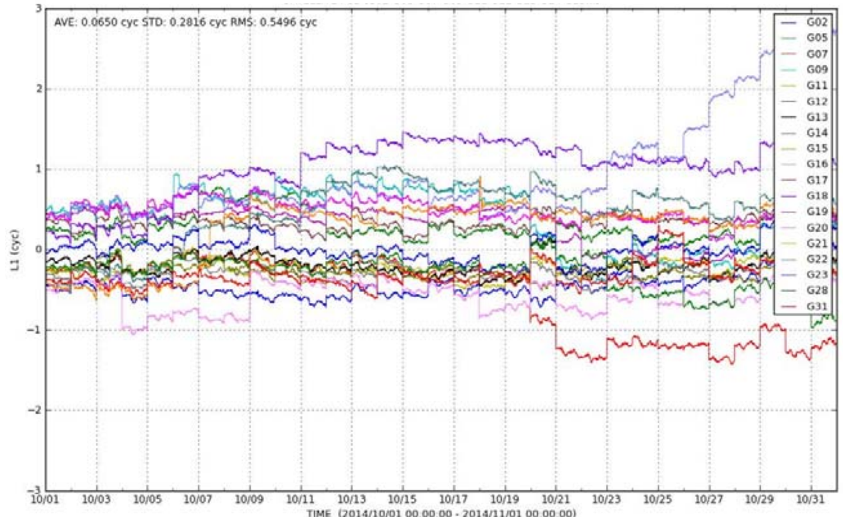

SD-WL-Ambiguity Residuals (cyc)

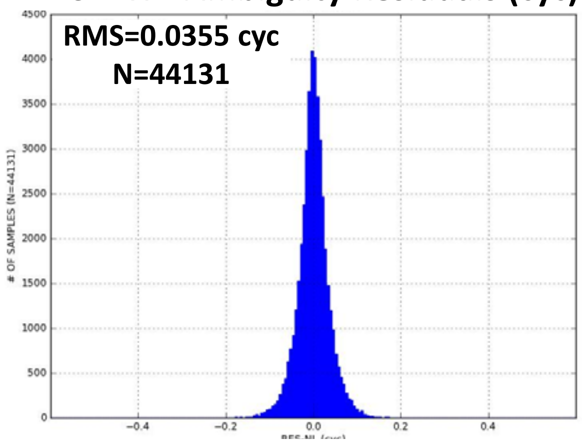

SD-NL-Ambiguity Residuals (cyc)

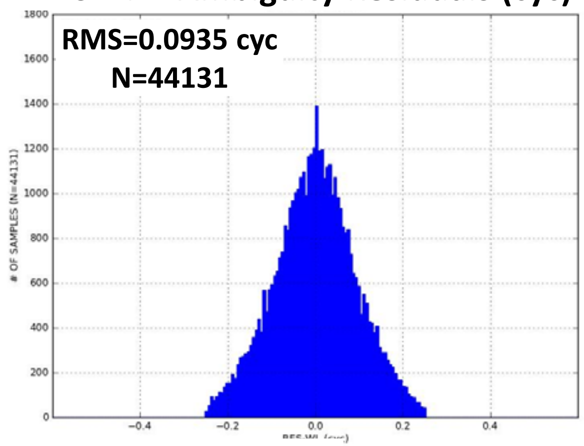

(MADOCA 0.7.2, GENFCB 1.2, GPS Block IIR, IIR-M, 19 satellites)

PPP-AR Example

PPP (w/o AR)

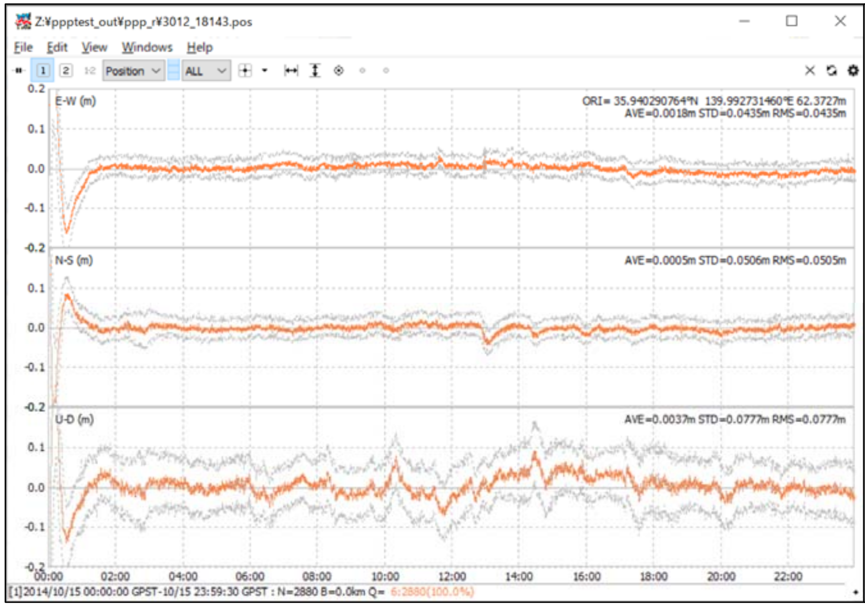

PPP-AR

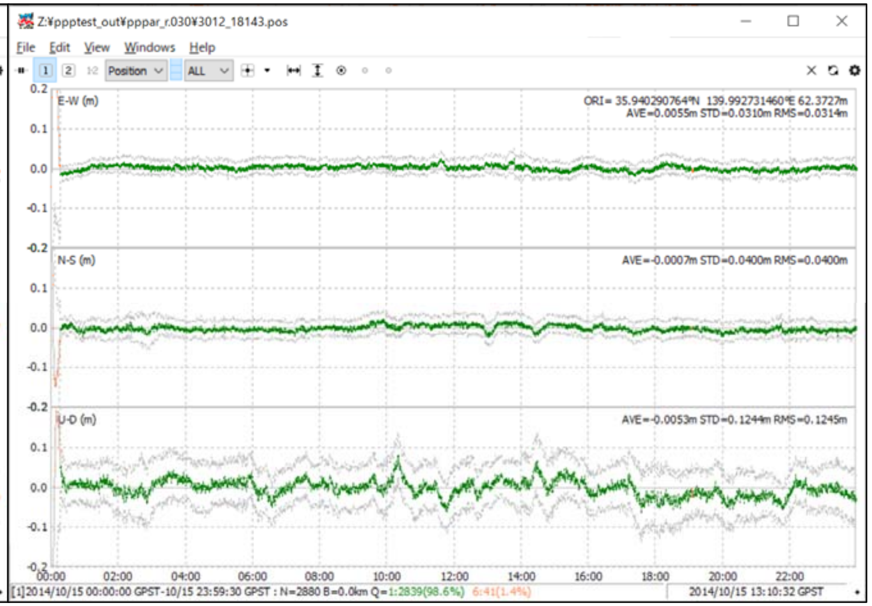

RMS Error: E 1.01, N 0.77, U 2.29 cm

RMS Error: E 0.67, N 0.72, U 2.02 cm

(Kinematic mode, First 1 H solutions excluded for convergence time)

● FLOAT ● FIXED

(MADOCA 0.7.2, GENFCB 1.2, RTKLIB 2.4.2, GEONET 3012, 2014/10/15 0:00:00-23:59:30 GPST)

Commercial PPP Services

Service	Provider	Supported GNSS	# of Ref. Stations	Comm. Link	Receivers	Accuracy
StarFire™ [1]	NAVCOM A John Deere Company (US)	GPS, GLO	> 40	3 GEO (L-band), IP	NavCom	< 5 cm
Seastar™ [2]	FUGRO (NED)	GPS, GLO, GAL, BDS (G4)	~ 80	6 GEO (L-band), IP (NTRIP)	Fugro	10 cm H 15 cm V (95%)
Apex/Ultra [3] **TerraStar®** [4]	veripos (UK)	GPS, GLO, GAL, BDS, QZS (Apex5)	~ 80	7 GEO (L-band)	VERIPOS, NovAtel [7], Septentrio [8], TOPCON [9], Hemisphere [10]	< 5 cm H < 12 cm V (95%)
CenterPoint RTX [5]	Trimble (US)	GPS, GLO, GAL, BDS, QZS	~ 100	6 GEO (L-band), IP (NTRIP)	Trimble, Qualcomm (?)	2 cm H 5 cm V (RMS)
magicGNSS [6]	gmv (Spain)	GPS, GLO, GAL, BDS, QZS	~ 80	IP (NTRIP)	(RTCM SSR)	5 cm H 8 cm V (RMS)
GEOFLEX [11]	geoflex (France)	GPS, GLO, (GAL, BDS)	~ 100	GEO, IP, GPRS/UMTS	(RTCM SSR)	4 cm (2D-95%)

[1] https://www.navcomtech.com, [2] https://www.fugro.com, [3] https://veripos.com, [4] https://www.terrastar.net, [5] https://positioningservices.trimble.com, [6] https://magicgnss.gmv.com, [7] https://www.notavel.com, [8] https://www.septentrio.com, [9] https://www.topconpositioning.com, [10] https://www.hemispheregnss.com, [11] http://www.geoflex.fr

PPP Service Performance

Figure 10 Accuracy (Canada) – GPS vs GPS+GLONASS

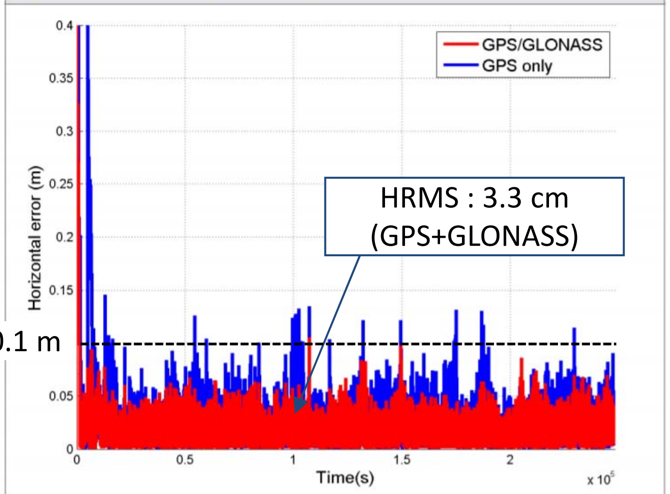

(3 days)

Table 5: Error Statistics at the Canada Station

PPP Correction Source	Horizontal RMS Error (cm)	Vertical RMS Error (cm)
TerraStar-C (GPS/GLONASS)	3.3	4.9
TerraStar-C (GPS only)	4.4	6.5

Figure 8 Convergence time (Canada) – GPS vs GPS+GLONASS

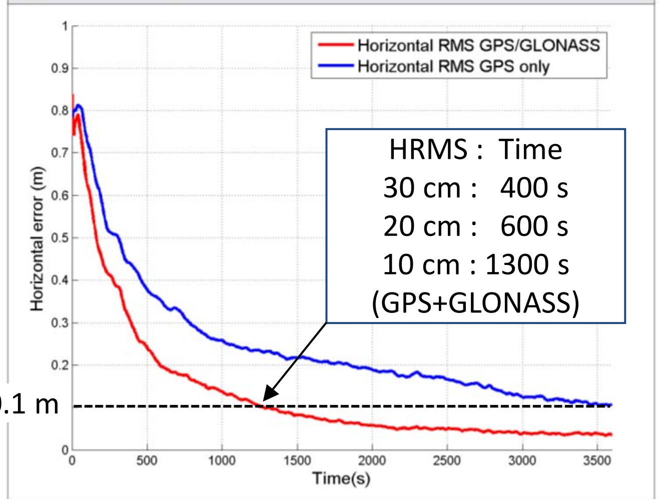

Figure 6 Re-convergence after 180 second signal outage

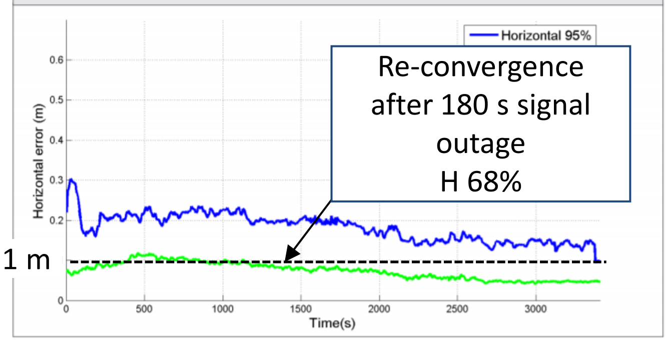

(NovAtel Correct with TerraStar-C in 2015)

[1] NovAtel White Paper, Precise Positioning with NovAtel CORRECT Including Performance Analysis, April 2015 (https://www.novatel.com/assets/Documents/Papers/NovAtel-CORRECT-PPP.pdf)

Faster Convergence for PPP-AR

PPP-RTK

- PPP-AR with local STEC and troposphere corrections
- High bandwidth required to support broad coverage larger than nation-wide
- Dense CORS N/W required for local corrections
- Supported by CLAS and some commercial PPP services

Fast-PPP [1]

- PPP-AR with global VTEC corrections
- Multi-layer model for global VTEC model
- Low bandwidth to transmit corrections for global coverage

Instantaneous cm-level PPP [2]

- No local or global TEC corrections
- Cascading PPP-AR with triple or quad frequencies (L1-L2-L5, E1-E5a-E5b-E6)

Fast-PPP [1]

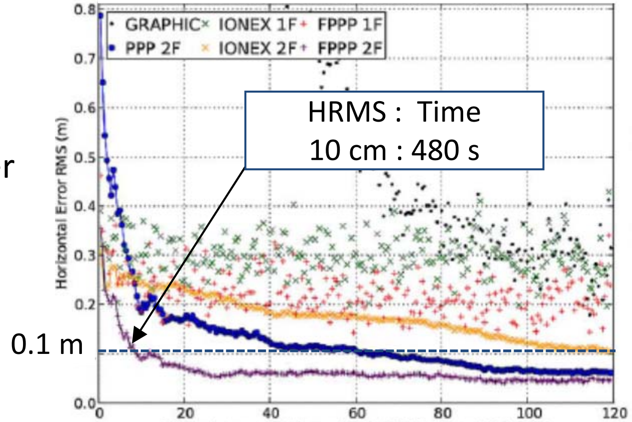

Instantaneous cm-level PPP [2]

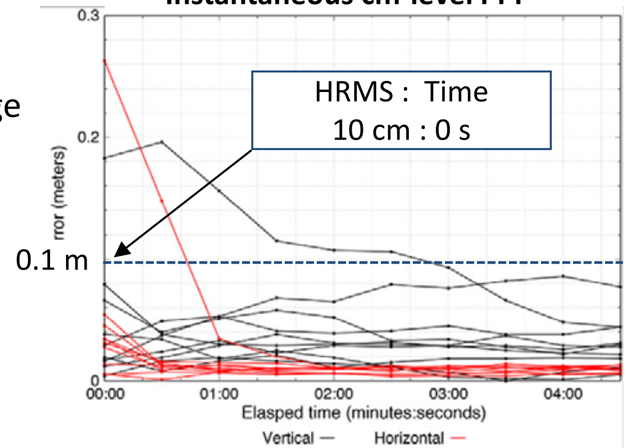

[1] A. R. Garcia et al., A worldwide ionospheric model for fast precise point positioning, IEEE Transaction on Geoscience and Remote Sensing, 2015

[2] D. Laurichesse and S. Banville, Innovation: Instantaneous centimeter-level multi-frequency precise point positioning, GPS World, 2018